



RESEARCH PAPER

The class II KNOX transcription factors KNAT3 and KNAT7 synergistically regulate monolignol biosynthesis in *Arabidopsis*

Wenqi Qin^{1,2}, Qi Yin^{1,2}, Jiajun Chen^{1,2}, Xianhai Zhao^{1,2}, Fengxia Yue³, Junbo He^{1,2}, Linjie Yang³, Lijun Liu⁴, Qingyin Zeng⁵, Fachuang Lu³, Nobutaka Mitsuda⁶, Masaru Ohme-Takagi⁷ and Ai-Min Wu^{1,2,*}

¹ State Key Laboratory for Conservation and Utilization of Subtropical Agro-bioresources, South China Agricultural University, Guangzhou 510642, China

² Guangdong Key Laboratory for Innovative Development and Utilization of Forest Plant Germplasm, College of Forestry and Landscape Architecture, South China Agricultural University, Guangzhou 510642, China

³ State Key Laboratory of Pulp and Paper Engineering, South China University of Technology, Guangzhou 510640, China

⁴ State Forestry and Grassland Administration Key Laboratory of Silviculture in downstream areas of the Yellow River, College of Forestry, Shandong Agriculture University, Taian 271018, Shandong, China

⁵ State Key Laboratory of Tree Genetics and Breeding, Chinese Academy of Forestry, Beijing 100091, China

⁶ Bioproduction Research Institute, National Institute of Advanced Industrial Science and Technology (AIST), Tsukuba 305–8566, Ibaraki, Japan

⁷ Green Biology Research Center, Saitama University, Saitama 338–8570, Japan

* Correspondence: wuaimin@scau.edu.cn

Received 12 February 2020; Editorial decision 20 May 2020; Accepted 22 May 2020

Editor: Simon Turner, University of Manchester, UK

Abstract

The function of the transcription factor *KNOTTED ARABIDOPSIS THALIANA7* (*KNAT7*) is still unclear since it appears to be either a negative or a positive regulator for secondary cell wall deposition with its loss-of-function mutant displaying thicker interfascicular and xylary fiber cell walls but thinner vessel cell walls in inflorescence stems. To explore the exact function of *KNAT7*, class II *KNOTTED1-LIKE HOMEOBOX* (KNOX II) genes in *Arabidopsis* including *KNAT3*, *KNAT4*, and *KNAT5* were studied together. By chimeric repressor technology, we found that both *KNAT3* and *KNAT7* repressors exhibited a similar dwarf phenotype. Both *KNAT3* and *KNAT7* genes were expressed in the inflorescence stems and the *knat3 knat7* double mutant exhibited a dwarf phenotype similar to the repressor lines. A stem cross-section of *knat3 knat7* displayed an enhanced irregular xylem phenotype as compared with the single mutants, and its cell wall thickness in xylem vessels and interfascicular fibers was significantly reduced. Analysis of cell wall chemical composition revealed that syringyl lignin was significantly decreased while guaiacyl lignin was increased in the *knat3 knat7* double mutant. Coincidentally, the *knat3 knat7* transcriptome showed that most lignin pathway genes were activated, whereas the syringyl lignin-related gene *Ferulate 5-Hydroxylase* (*F5H*) was down-regulated. Protein interaction analysis revealed that *KNAT3* and *KNAT7* can form a heterodimer, and *KNAT3*, but not *KNAT7*, can interact with the key secondary cell wall formation transcription factors *NST1/2*, which suggests that the *KNAT3–NST1/2* heterodimer complex regulates *F5H* to promote syringyl lignin synthesis. These results indicate that *KNAT3* and *KNAT7* synergistically work together to promote secondary cell wall biosynthesis.

Keywords: Cell wall, *KNAT3*, *KNAT7*, monolignol, lignin, secondary cell wall, xylem.

Introduction

Lignin is one of the major structural components in plant secondary cell walls and provides mechanical strength and stiffness to the plant cells (Boerjan *et al.*, 2003; Cosgrove and Jarvis, 2012). Three types of lignin subunits, i.e. *p*-hydroxyphenyl (H), guaiacyl (G), and syringyl (S), are derived from oxidative polymerization of three monolignols, *p*-coumaryl, coniferyl, and sinapyl alcohols, respectively (Boerjan *et al.*, 2003).

Phenylalanine is used as substrate to produce hydroxycinnamoyl-CoA esters in the phenylpropanoid pathway involved in monolignol biosynthesis. At least 11 enzymes are involved in catalysing monolignol biosynthesis: phenylalanine ammonia lyase (PAL), cinnamate 4-hydroxylase (C4H), 4-coumarate CoA ligase (4CL), hydroxycinnamoyl CoA:shikimate hydroxycinnamoyl transferase (HCT), *p*-coumaroyl shikimate 3'-hydroxylase (C3H), caffeoyl CoA O-methyltransferase (CCoAOMT), ferulate 5-hydroxylase (F5H), caffeic acid O-methyltransferase (COMT), cinnamoyl CoA reductase (CCR), cinnamyl alcohol dehydrogenase (CAD), and caffeoyl shikimate esterase (CSE) (Boerjan *et al.*, 2003; Bonawitz and Chapple, 2010; Vanholme *et al.*, 2013). Of these enzymes, F5H is the key catalyst in the synthesis of S-lignin. A complicated transcriptional network regulates secondary cell wall formation, with the top-level regulators VASCULAR RELATED NAC-DOMAIN PROTEIN6 (VND6), VND7, and NAC (NAM, ATAF1/2, and CUC2) transcription factors, second-level regulators MYB46 and MYB83, and a battery of downstream transcription factors, namely MYB20, MYB42, MYB43, MYB52, MYB54, MYB58, MYB63, MYB69, MYB85, MYB103, and KNOTTED ARABIDOPSIS THALIANA7 (KNAT7). The transcriptional regulation of lignin biosynthesis has revealed that some MYB transcription factors can activate monolignol pathway genes directly by binding to the AC-rich elements of their promoters (Lacombe *et al.*, 2000; Patzlaff *et al.*, 2003; Goicoechea *et al.*, 2005; Zhou *et al.*, 2009). The promoters of PAL, 4CL, C3H, CCoAOMT, CCR, and CAD all contain the conserved AC elements, while the promoters of C4H and COMT contain degenerated AC elements (Zhou *et al.*, 2009; Zhao and Dixon, 2011). Therefore, all those genes might be directly regulated by the known lignin-specific transcription factors, such as *AtMYB58* and *MYB63*. However, F5H, the key gene for S-lignin biosynthesis, neither contains AC-rich elements nor is regulated by the lignin-specific transcription factors (Zhou *et al.*, 2009; Zhao and Dixon, 2011). Although it is reported that the *Medicago* F5H gene is directly regulated by SND1 (NST3) (Zhao *et al.*, 2010), evidence for such regulation in Arabidopsis is lacking (Öhman *et al.*, 2013). The molecular regulation of F5H in Arabidopsis is still elusive.

KNAT7 has been reported to function as a repressor of secondary cell wall formation, and its disruption results in thicker interfascicular fiber walls in Arabidopsis (Li *et al.*, 2012). The known KNAT7 interactors, such as OVATE FAMILY PROTEIN4 (OFP4), BELL-LIKE HOMEODOMAIN6 (BLH6), and MYB75 (Hackbusch *et al.*, 2005; Bhargava *et al.*, 2010; Li *et al.*, 2011; Liu *et al.*, 2014), are negative regulators of secondary wall formation. Paradoxically, the *knat7* mutant had

thinner vessel cells (Li *et al.*, 2012), and there was reduced secondary wall thickness in KNAT7 dominant repressing transgenic plants (Zhong *et al.*, 2008). Our recent study revealed that KNAT7 positively affects xylan (the important composition of hemicellulose) biosynthesis (He *et al.*, 2018). These results imply that KNAT7 has complicated functions with regard to specific cell types or interacting regulators.

KNAT7 is one of the *KNOTTED1-LIKE HOMEBOX* (KNOX) genes, which belong to the plant-specific Three Amino Acid Loop Extension (TALE) homeodomain superfamily (Hake *et al.*, 2004; Hay and Tsiantis, 2010). KNOX genes can be grouped into two classes: KNOX I (*SHOOTMERISTEMLESS* (STM), *BREVIPEDICELLUS* (BP), KNAT2, and KNAT6) and KNOX II (KNAT3, KNAT4, KNAT5, and KNAT7) (Kerstetter *et al.*, 1994; Mukherjee *et al.*, 2009). KNAT3, KNAT4, and KNAT5 function redundantly to influence leaf morphology in *Arabidopsis* (Furumizu *et al.*, 2015). As they are KNOX II clade members, it would be interesting to explore whether KNAT3, KNAT4, and KNAT5 have redundant functions with KNAT7 on secondary wall formation in inflorescence and stem, and thus to interpret the diverse and paradoxical roles of KNAT7.

Here, we report that the loss-of-function *knat3 knat7* double mutant displays an enhanced irregular xylem (*irx*) phenotype including thinner vessel and interfascicular cell wall thickness. The actual chemical composition revealed an increase in G-lignin and a decrease in S-lignin. RNA-seq results displayed significant down-regulation of *F5H*. A protein interaction assay identified that KNAT3 and KNAT7 form a heterodimer, and KNAT3, but not KNAT7, can interact with NST1 and NST2. Altogether, our results show that KNAT3 and KNAT7 form a complex to paradoxically regulate secondary cell wall formation in different tissue.

Materials and methods

Plant material and growth conditions

Arabidopsis ecotype Columbia (Col-0) was used as the WT plant and for transgenic plant experiments. Plants were grown on soil with supplemental lighting with a photoperiod of 16 h light–8 h dark and light intensity and temperature of 120 $\mu\text{mol m}^{-2} \text{s}^{-1}$ and 22 °C, respectively. The T-DNA insertion mutant allele of *myb103-1* (AT1G63910 SALK_210187C), *myb103-2* (AT1G63910 SAIL_337_C03), and KNAT3 (AT5G25220 SALK_136464) and KNAT7 (AT1G62990 SALK_110899), designated *knat3* and *knat7*, were identified using the SIGnal database (<http://signal.salk.edu/>), and seeds were obtained from the *Arabidopsis* Biological Resources Center (ABRC, Columbus, OH, USA). KNAT3 and KNAT7 gene-specific primers used for PCR genotyping are listed in Supplementary Table S1 at JXB online.

Plasmid constructs and generation of transgenic plants

Promoter fragments of 2 kb, 2.6 kb upstream of the ATG start codons of KNAT3 and KNAT7 were designed. The promoter fragments were cloned into the pDONR207 vector and then transferred into pGWB3 (Nakagawa *et al.*, 2007) and all constructs were used to transform WT *Arabidopsis*. Both KNAT3 and KNAT7 coding regions were individually cloned into pDONR207 and then recombined into pEarleyGate100. Chimeric repressor constructs were prepared by inserting the coding

sequence of *KNAT3* and *KNAT7* with one extra guanine nucleotide at the 5' end into the *Smal* site of p35S:SRDXG vector and then transferred into vector pBCKH (Mitsuda *et al.*, 2006), in which a chimeric repressor was produced by fusion transcription factors to the plant-specific ERF associated Amphiphilic Repression (EAR) repression domain (LDLDLELRLGFA). Finally, all DNA constructs were verified by DNA sequencing analysis and were electroporated into *Agrobacterium tumefaciens* GV3101. Transformation of WT plants and the *knat3 knat7* double mutant was done using the floral dip method (Clough and Bent, 1998). Transgenic lines were screened on 1/2 MS plates plus 50 mg ml⁻¹ kanamycin or glufosinate ammonium at 2000× dilution (Sigma).

β-Glucuronidase staining

β-Glucuronidase (GUS) activity was examined in 40 mm sections of 6-week-old inflorescence stems. Sections were washed three times with phosphate-buffered saline (pH 7.0), and incubated with GUS staining solution (100 mM Na₃PO₄, pH 7.0, 1 mM EDTA, 1 mM potassium ferrocyanide, 1 mM potassium ferricyanide, 1% Triton X-100, and 1 mg ml⁻¹ 5-bromo-4-chloro-3-indolyl β-D-glucuronide (X-Gluc)) for 8 h to overnight at 37 °C in dark. After decolorization in 95% or 75% ethanol (Jefferson *et al.*, 1987; Wu *et al.*, 2009), the sections were observed under a light microscope.

Sectioning of stems

Segments were cut from the basal internode of stems of 6-week-old plants. A Leica VT1000S vibrating-blade microtome was used to cut 40 mm sections by using 3% agarose as support. Phloroglucinol-HCl Staining was performed; the sections were stained for 5 s in 3% phloroglucinol, then were washed out followed by the addition of concentrated HCl (37 M), and then observed using a light microscope. For Mäule staining, 0.5% potassium permanganate solution was added to the sections for staining; the solution was washed out and then distilled water was added to rinse out the potassium permanganate solution; finally, 3% HCl was added and it was incubated for 3–5 min until the deep brown color was discharged from the sections. After pipetting out all the HCl solution, concentrated ammonium hydroxide solution was added immediately (Pradhan and Loque, 2014). Then the sections were observed under bright field microscopy (BX43F; Olympus, Japan). Finally, cell wall thickness was measured by the microscope's software and combined with the software ImageJ.

Cell wall preparation and lignin analysis

To measure total lignin content and monomeric lignin composition, 8-week-old mature stems were collected, with three biological replicates, each replicate having at least six plants. After ball-milling into powder, wax was removed using a Soxhlet extractor. The powder was incubated with 4% diluted sulfuric acid at 121 °C for 60 min to completely hydrolyse. The hydrolysate was filtered to determine the acid-soluble lignin, and the residue was measured for acid-insoluble lignin. Determination and calculation methods were the same as previously described (Wang *et al.*, 2019). Thioacidolysis was used to analyse lignocellulosic samples and 2D heteronuclear single quantum coherence (HSQC) spectroscopy was performed following the methods used by Yue *et al.* (2012), Kim and Ralph (2010), and Mansfield *et al.* (2012).

RNA-seq

Six-week-old *Arabidopsis* stem bases of Col-0 and *knat3 knat7* plants were collected and ground to powder in liquid nitrogen. Total RNA extraction and RNA-seq were performed by the Biomarker Technologies Corporation (Beijing, China). Differential gene expression analysis and Gene Ontology enrichment analysis were performed using BMKcloud (international.biocloud.net). The TAIR10 genome was used as the *Arabidopsis* reference genome (www.arabidopsis.org) and the RNA-seq data were submitted to <http://bigd.big.ac.cn/gsa/> with submission number CRA002075.

RT-PCR and qRT-PCR analyses

Total RNA was isolated using a plant RNA kit (Omega, Norcross, GA, USA) according to the manufacturer's instructions. First-strand cDNA synthesis was carried out with approximately 2 µg RNA using the Primer Script RT Reagent Kit with gDNA Eraser (Takara, Kyoto, Japan). RT-PCR was conducted with first-strand cDNA as the template, and amplified fragments were confirmed using agarose gel electrophoresis. The qRT-PCR was performed with the SYBR Premix Ex Taq II (Takara) on a LightCycler480 Real-Time PCR System (Roche, Basel, Switzerland). Primers used for RT-PCR and qRT-PCR are listed in Supplementary Table S1.

Yeast two-hybrid assays

To test the interaction between KNAT3, KNAT7, NST1, and NST2 proteins, the bait constructs pDEST32-KNAT3 and pDEST32-KNAT7 were generated by LR reaction between pDONR207-KNAT3, pDONR207-KNAT7 plasmids and pDEST32 (Thermo Fisher Scientific). The prey constructs pDEST22-NST1, pDEST22-NST2, pDEST22-KNAT3, and pDEST22-KNAT7 were generated by LR reaction between pDONR207-NST1, pDONR207-NST2, pDONR207-KNAT3, pDONR207-KNAT7, and pDEST22 (Thermo Fisher Scientific). Bait plasmids and prey plasmids or blank pDEST22 were co-transformed into yeast strain AH109. Medium supplemented with SD-Leu-Trp-His and 2.5 mM 3-amino-1,2,4-triazole was used for selection (Tao *et al.*, 2013).

Yeast one-hybrid assay

To test whether KNAT3 and KNAT7 could bind the promoter of the *F5H* gene directly, a yeast one-hybrid assay was performed. The coding sequences (CDS) of *KNAT3* and *KNAT7* genes were amplified by PCR and were inserted into *Eco*RI/*Xho*I sites of pB42AD vector. The 2171 bp promoter region of the *F5H* gene was amplified by PCR and inserted to *Eco*RI/*Xho*I sites of pLacZi2µ vector. All the constructions were confirmed by sequencing. The corresponding pB42AD and pLacZi2µ fusion constructions were co-transformed into yeast strain EGY48 containing p8op-LacZ plasmid. The transformants were spread on SD-/His-Trp-Ura dropout plates. After 3 d growth at 30 °C, the transformants were copied to SD-/His-Trp-Ura dropout plates containing 80 mg l⁻¹ X-gal for blue color development. pB42AD-CCA1 and pLacZi2µ-proELF4 combination from (Zhao *et al.*, 2018) was used as positive control.

Firefly split luciferase complementation imaging

The full-length CDSs of *KNAT3*, *KNAT7*, *NST1*, and *NST2* were amplified from *Arabidopsis* cDNA and then cloned into pDONR207 to generate the pENTRY construct. nLUC-KNAT3 or cLUC-KNAT7/NST1/NST2 was generated by LR reactions between pCB1300-nLUC-GW or pCB1300-cLUC-GW and pDONR207-NST1, pDONR207-NST2, pDONR207-KNAT3, pDONR207-KNAT7 (Thermo Fisher Scientific). These plasmids were transformed into *Agrobacterium* strain GV3101. Different combinations of plasmids were co-infiltrated into tobacco (*Nicotiana benthamiana*) leaves. The empty pCB1300-BD-nLUC and pCB1300-cLUC-GW vectors were used as negative controls. After incubation in dark for 24 h and then in light for 72 h, the tobacco leaves were sprayed with 100 mM D-luciferin and kept in dark for 10 min (Han *et al.*, 2019). The fluorescence was detected using a low-light cooled charge-coupled device (CCD) imaging apparatus (NightOWL818 II LB983) with indiGO software.

Transactivation analyses

A 2171bp promoter sequence of *F5H* was amplified from *Arabidopsis* genomic DNA, then recombined into pGreen II 0800-LUC vector, and used as reporter plasmids (Hellens *et al.*, 2005). The coding sequence of *KNAT3/KNAT7* was amplified by PCR, inserted into pGreen II 62-SK, and used as an effector plasmid. The effector and reporter were co-transfected into *Arabidopsis* leaf protoplasts (Yoo *et al.*, 2007). After

placing them under low-light conditions for 14–16 h, the protoplasts were lysed and the supernatants were assayed for LUC and REN activities with the Dual-Luciferase Reporter Assay System (Promega, Madison, WI, USA). The LUC/REN ratio indicates transcriptional activity.

Co-immunoprecipitation and immunoblot analyses

Total proteins from *Nicotiana benthamiana* were extracted using IP buffer containing 150 mM NaCl, 50 mM Tris-HCl (pH 7.5), 5 mM EDTA, 10% glycerol, 1% Triton X-100, 0.2% NP-40, 5 mM DTT, and 1× complete protease inhibitor cocktail. Anti-FLAG M2 Magnetic Beads (Sigma, M8823) were used for immunoprecipitation for hemagglutinin (HA)- and FLAG-tagged proteins. The affinity beads were washed with washing buffer (150 mM NaCl, 50 mM Tris-HCl pH 7.5, 5 mM EDTA, 1% Triton X-100, 0.2% NP-40, and 1× complete protease inhibitor cocktail). The protein extract was incubated with the affinity beads for 4 h at 4 °C with gentle mixing to capture the proteins. Anti-FLAG (Abmart, M20008) and anti-HA (Abmart, M20003) antibodies from mice were used to detect input proteins; anti-FLAG (Sigma, F7452) and anti-HA (Sigma, H6908) antibodies from rabbits were used to detect immunoprecipitated proteins. Immunoblots were performed according to the enhanced chemiluminescence western blotting procedure.

Results

Chimeric KNAT3 and KNAT7 repressors induced similar dwarf phenotype

To examine the paradox of KNAT7 negatively and positively regulating secondary cell wall biosynthesis (Zhong *et al.*, 2006, 2007, 2008; Li *et al.*, 2011, 2012; Zhong and Ye, 2012; He *et al.*, 2018), the KNOX II proteins KNAT3, KNAT4, KNAT5, and KNAT7 (Furumizu *et al.*, 2015) were fused with the EAR-motif repressor domain SRDX (Hiratsu *et al.*, 2003, 2004), which converted the individual KNOXII transcription factors into dominant repressors. The chimeric KNOX II repressor cassettes, driven by the cauliflower mosaic virus (CaMV) 35S promoter (p35S:KNOX II-SRDX), were expressed in Arabidopsis (see Supplementary Fig. S1A). Among all four KNOX II-SRDX transgenic plants, only p35S:KNAT3-SRDX and p35S:KNAT7-SRDX showed morphological resemblance, displaying a similar dwarf and bush phenotype (Supplementary Fig. S1B), which suggests a probable functional redundancy of KNAT3 and KNAT7 in inflorescence stems.

KNAT3 and KNAT7 were co-expressed in the interfascicular fiber and xylem

To validate the speculated functional redundancy of KNAT3 and KNAT7 in inflorescence stems, we first examined the expression of *KNAT3* and *KNAT7* genes in Arabidopsis. The relative transcription levels of *KNAT3* and *KNAT7* in different tissues were detected by qRT-PCR. The results showed that the expression level of *KNAT7* in the stem was much higher than that of *KNAT3*, while compared with *KNAT7*, the expression level of *KNAT3* in the cauline and senescent leaves was higher (Fig. 1A). To further check expression patterns of *KNAT3* and *KNAT7* in inflorescence stems, the promoter regions of *KNAT3* or *KNAT7* were fused with the *GUS* gene; the resultant vectors p*KNAT3*:GUS and p*KNAT7*:GUS were then

transferred into wild-type plants. Despite the p*KNAT3*:GUS showing diffusion in phloem and other cells, GUS staining for both p*KNAT3*:GUS and p*KNAT7*:GUS was observed in both xylem and interfascicular fiber cells (Fig. 1D, E). These results confirmed that *KNAT3* and *KNAT7* were co-expressed in the inflorescence stems.

knat3 knat7 double mutant exhibits severe irregular xylem phenotype

To further analyse the functional redundancy between KNAT3 and KNAT7, the double mutant was obtained by crossing *knat3* (SALK_136464) and *knat7* (SALK_110899) single mutants. RT-PCR analysis showed that transcript fragments of KNAT3 and KNAT7 in *knat3* and *knat7* single mutants were not amplified (Fig. 2C), indicating that KNAT3 and KNAT7 cannot form intact mRNA due to T-DNA insertions, and thus these two lines were functionally knock-out mutants. Morphologically, *knat3* and *knat7* single mutants had a similar height to the wild type (WT), while the *knat3 knat7* double mutant was significantly shorter than the WT (Fig. 2D, E).

To elucidate the reason for the difference in height between *knat3* and *knat7* mutant combinations, cross-sections were taken from the base of the inflorescence stems of 6-week-old WT, *knat3*, *knat7*, and *knat3 knat7* plants. *knat3*, like the WT, exhibited a normal vessel phenotype, and *knat7* showed slightly weak irregular vessels (Fig. 3A–C), whereas severe irregular xylem vessels were clearly observed in the *knat3 knat7* double mutants (Fig. 3D). The thickness of xylem (vessel and xylary) and interfascicular fiber cell walls of WT, *knat3*, *knat7*, and *knat3 knat7* was further measured. Compared with WT, *knat7* had thicker interfascicular fiber cell walls but thinner vessel and xylary cell walls in inflorescence stems (Fig. 3E–G), which is consistent with previous reports (Li *et al.*, 2012; He *et al.*, 2018). On the contrary, the cell wall thickness of interfascicular fibers was reduced in *knat3*, while all the vessel, xylary, and interfascicular fiber cell walls were significantly thinner in the *knat3 knat7* double mutant. These results indicate that KNAT3 and KNAT7 have functional redundancy in regulating at least the xylem vessel and xylary secondary cell wall development.

Complementation was performed to investigate whether the phenotype of the *knat3 knat7* double mutant was indeed caused by knockout of the corresponding genes. The full-length coding sequences of KNAT3 and KNAT7 were fused with CaMV35S promoter and transferred to the *knat3 knat7* mutant. The transgenic lines fully rescued the dwarfism and the irregular xylem phenotype of the mutant (Figs 2F, 3H). These results confirm that the phenotype of the *knat3 knat7* mutant is indeed caused by the loss of function of KNAT3 and KNAT7.

KNAT3 and KNAT7 synergistically regulate syringyl lignin biosynthesis

Mäule staining was performed on stem cross-sections of p35S:KNAT3-SRDX and p35S:KNAT7-SRDX repressor transgenic plants to examine chemical changes in cell wall composition of *knat3* and *knat7* mutants (see Supplementary

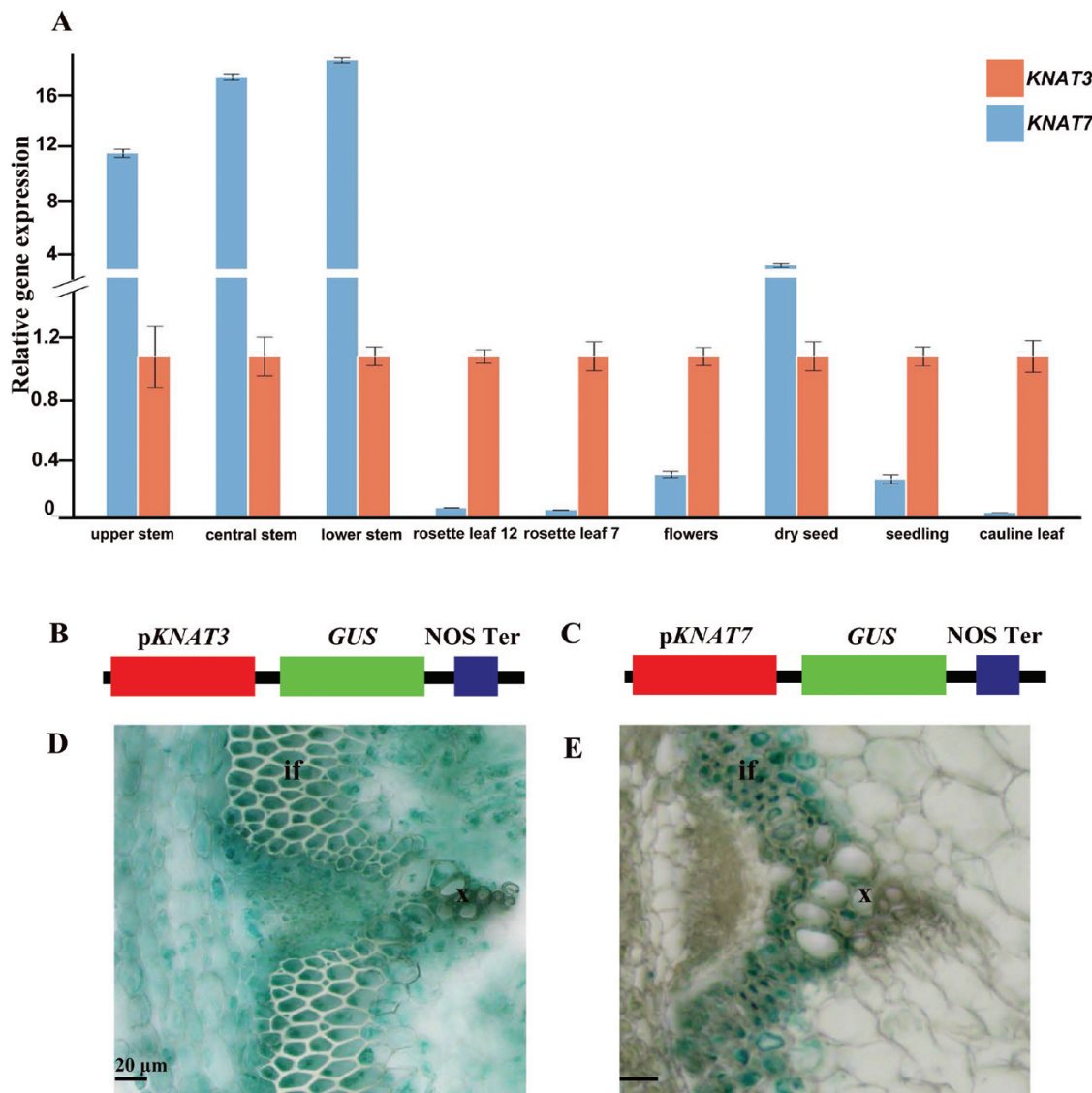


Fig. 1. The expression pattern of KNAT3 and KNAT7. (A) Relative expression levels of KNAT3 and KNAT7 at different tissues in 6-week-old Arabidopsis measured by qRT-PCR. Column height indicates the mean value \pm SD of the sample expression; $n=4$. The expression level of KNAT3 in the WT was assigned a value of 1, and ACT8 was used as an internal reference. (B, C) Schematic diagrams of the pKNAT3:GUS and pKNAT7:GUS cassette, respectively. On the left is the promoter, in the middle the GUS gene, and on the right the terminator. (D, E) GUS staining for pKNAT3:GUS (D) and pKNAT7:GUS (E); samples were from the base of the 6-week-old stem. If, interfascicular fibers; x, xylem. Scale bar: 20 μ m. (This figure is available in color at JXB online.)

Fig. S2). The wild-type xylem was stained bright red, the p35S:KNAT7-SRDX xylem was stained weak brown-red, and the p35S:KNAT3-SRDX xylem was stained yellow-brown (**Supplementary Fig. S2**). These results indicate that the synthesis of S-lignin might be significantly inhibited in KNAT3 repressor transgenic plants.

To verify whether the lignin defect in the chimeric KNAT3 and KNAT7 repressors corresponds to the *knat3 knat7* mutation, the lignin content of KNAT3 and KNAT7 mutants was further determined. The results showed that acid-soluble lignin in the *knat3* and *knat3 knat7* mutants was significantly reduced compared with the WT. However, no significant changes were found in the acid-insoluble lignin and total amount of lignin in the *knat3*, *knat7*, and *knat3 knat7* mutants compared with WT (**Fig. 4A–C**). Furthermore, Mäule staining showed that the

stem section of the *knat3 knat7* mutant stained yellow-brown (**Fig. 4D–G**), which is consistent with the observation in domain repressor plants. The stem cross-sections of KNAT3 and KNAT7 complementation plants in the *knat3 knat7* double mutant rescued the color changes from yellow-brown to bright-red (see **Supplementary Fig. S3**). These results indicate a decrease in S-lignin in the *knat3 knat7* double mutant.

To determine the amount of S-lignin reduction, GC-MS was used to detect the content of S- and G-lignin monomers (**Table 1**). G-lignin was significantly reduced in *knat3*, but significantly increased in *knat7* and *knat3 knat7*. Due to significant down-regulation of both G-lignin and S-lignin in *knat3*, the S/G ratio showed no change whereas the S/G ratio in *knat7* decreased because of an increase in G-lignin and a slight decrease in S-lignin (**Table 1**). Furthermore, the S-lignin

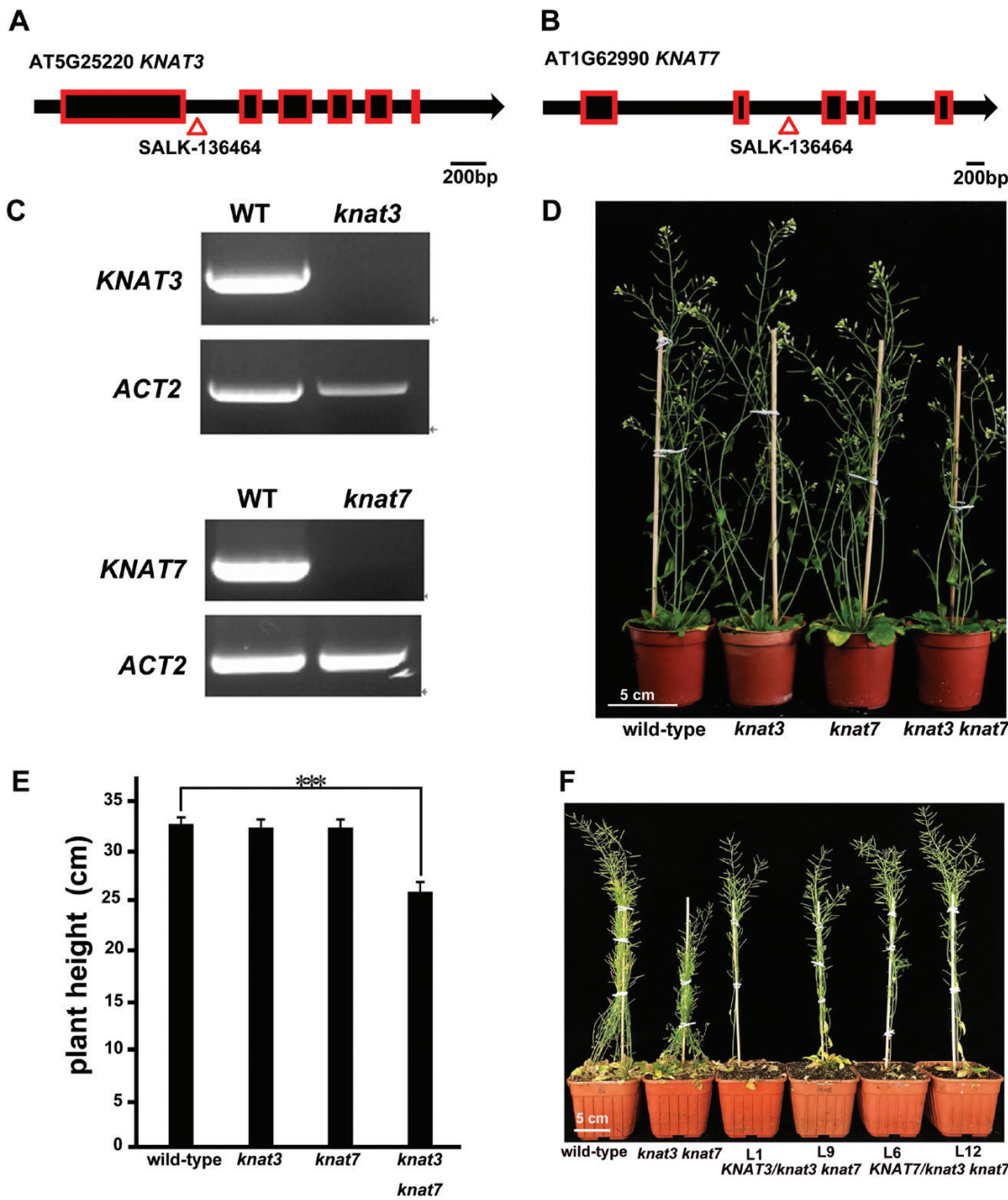


Fig. 2. The morphology of *knat3 knat7* double mutant. (A, B) Schematic diagrams representing the T-DNA insertion positions of *knat3* (A) and *knat7* (B). The boxes and lines indicate exons and introns, respectively, and the triangle indicate the T-DNA insertion position labeled with the Salk number. (C) RT-PCR results showed that the fragments of *knat3* and *knat7* were not amplified in the corresponding mutants compared with WT; *ACT2* was used as an internal reference gene. (D) The height of 6-week-old WT, *knat3*, *knat7*, and *knat3 knat7*. Scale bar: 5 cm. (E) Compared with the WT, there was no significant difference in the height of *knat3* and *knat7*, but the height of *knat3 knat7* was significantly shorter at the same stages. Data are means with SD of 10 plants. ***Significant difference at $P < 0.01$ compared with wild-type plants, by *t*-test. (F) Complementation of *KNAT3* and *KNAT7* can rescue the height of *knat3 knat7*. (This figure is available in color at JXB online.)

content was further reduced by about 80% in the *knat3 knat7* double mutant compared with WT, which resulted in an 84% reduction of the S/G ratio in *knat3 knat7*. Additional 2D HSQC spectra of WT and *knat3 knat7* cell wall samples were collected to determine the lignin differences (Fig. 4H). The correlations in the HSQC spectra of whole cell wall preparations were assigned by comparison with published data (Kim and Ralph, 2010; Mansfield *et al.*, 2012). As shown in Fig. 4H, both G- and S-lignin signals were detected in the WT cell

walls, although the amount of S units was much lower than that of G units, which is consistent with thioacidolysis analysis (Table 1). However, in HSQC spectra of *knat3 knat7*, correlations of the S unit ($S_{2/6}$) were completely absent, while the correlations of G unit and H unit lignin subunits were much stronger than those of WT, which indicates a much higher amount of G-lignin in *knat3 knat7*. Overall, 2D HSQC confirmed an increase in G-lignin and a decrease in S-lignin in the *knat3 knat7* mutant.

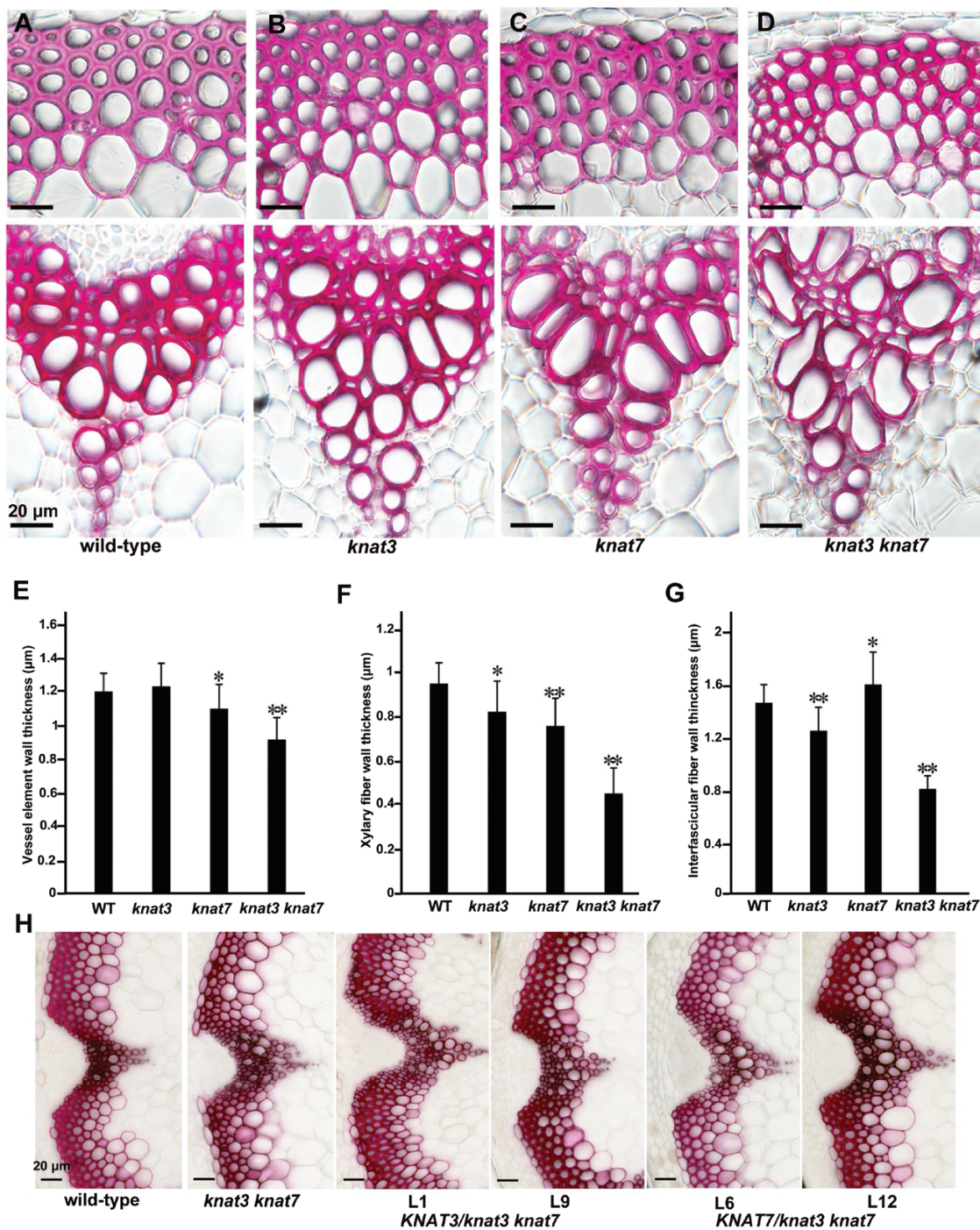


Fig. 3. The *knat3 knat7* double mutant shows severe irregular xylem. (A–D) Cross-sections of 6-week-old *Arabidopsis* base stems stained with phloroglucinol: (A) WT, (B) *knat3*, (C) *knat7*, (D) *knat3 knat7*. The upper panel shows the interfascicular fiber structure, and the lower panel shows the xylem tissue. Scale bar: 20 µm. (E–G) Cell wall thickness of different cells: vessel cell (E), xylary fiber cell (F), and interfascicular fiber cell (G). Data are mean with SD of 50 cell wall thicknesses. Significant difference compared with wild-type plants: * $P<0.05$, ** $P<0.01$; *t*-test. (H) Cross-sections of complementation plant by overexpressed *KNAT3* and *KNAT7* in *knat3 knat7* double mutant. (This figure is available in color at JXB online.)

The key S-lignin biosynthetic gene F5H was down-regulated in *knat3 knat7* mutant

To further explain the decrease of S-lignin in the *knat3 knat7* mutant, the main stems of 6-week-old WT and *knat3 knat7* mutant were collected for RNA sequencing. Data analysis showed that the differentially expressed genes were

significantly enriched in the phenylalanine metabolic pathway (see Supplementary Fig. S4), which is consistent with the phenotype of *knat3 knat7* mutant showing a significant decrease in the proportion of lignin S/G. Interestingly, the expression profiles of lignin metabolic pathway genes *CCR*, *COMT*, *CCoAOMT*, and *CAD* were up-regulated (Fig. 5A)

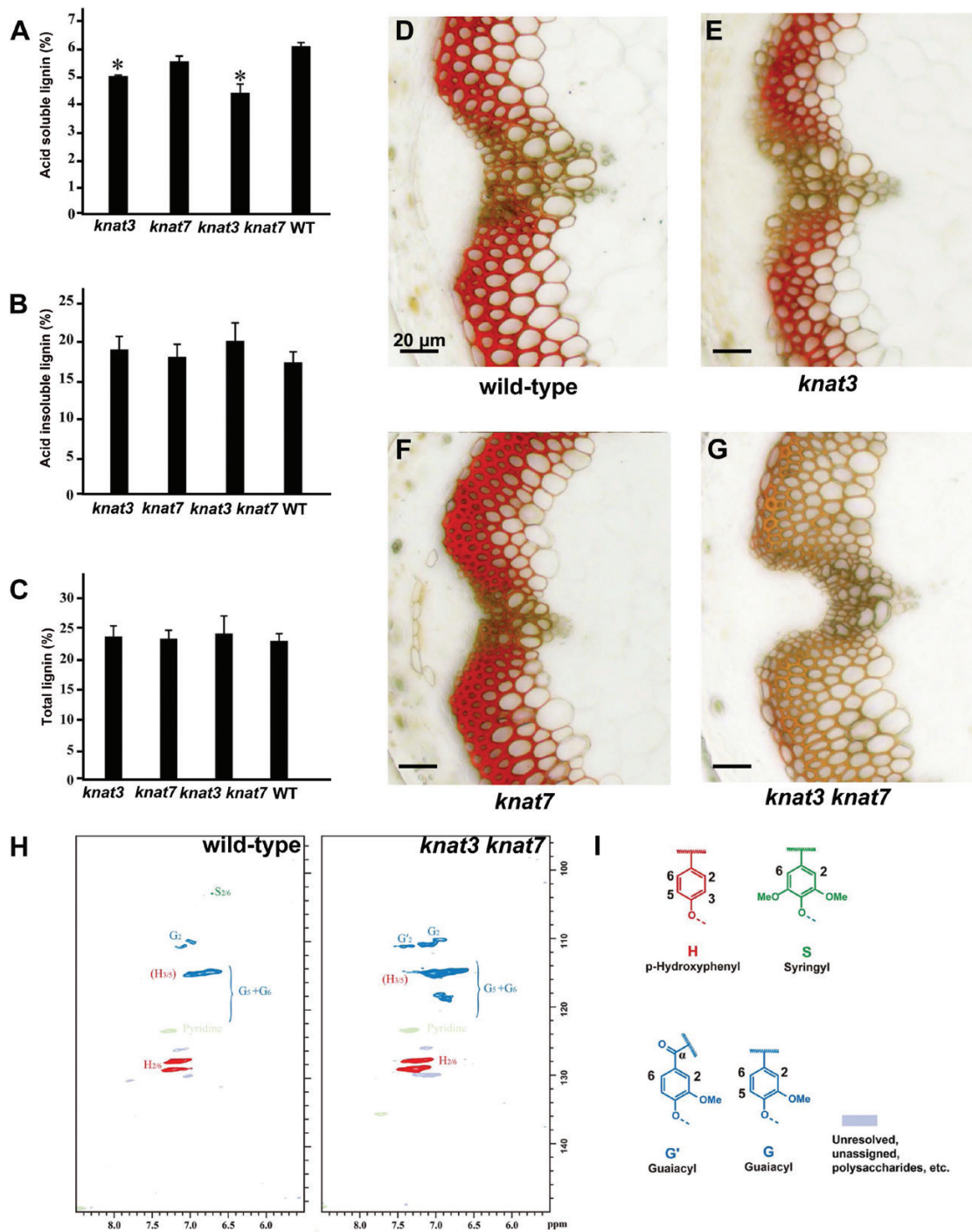


Fig. 4. Lignin content and Mäule staining of WT, *knat3*, *knat7*, and *knat3 knat7*. (A–C) Percentage content of acid-soluble lignin (A), acid-insoluble lignin (B), and total lignin (C) in the main stem of 8-week-old plants. Three biological replicates were included, and the significance analysis was based on Student's *t*-test. *Significant difference at $P < 0.05$ compared with WT plants. (D–G) Cross-sections from the base of 6-week-old stem with Mäule staining. It can be observed that *knat3 knat7* and WT were differentially stained. Scale bar: 20 μm . (H) Aromatic regions of 2D ^{13}C - ^1H correlation (HSQC) spectra from cell wall gels from various samples in DMSO- d_6 /pyridine- d_5 (4:1). The data showed that S-lignin decreased and G-lignin increased in *knat3 knat7*. (I) Chemical formulae corresponding to the different components in (H). (This figure is available in color at JXB online.)

and expression levels of *4CL1* and *F5H* were down-regulated. The increasing G-lignin content in *knat3 knat7* could be due to the activation of lignin pathway genes, such as G-lignin-related *CCoAOMT*. Because *F5H* is a key enzyme for the synthesis of S-lignin (Franke *et al.*, 2000; García *et al.*, 2014), the

reduced *F5H* expression might be attributed to the decrease of S-lignin content in the *knat3 knat7* mutant. Furthermore, the RNA-seq results were verified by qRT-PCR analysis of lignin biosynthetic genes in WT and *knat3 knat7* mutant, in which *F5H* expression was reduced by 77% (Fig. 5B).

Table 1. Determination of lignin monomer

Sample	G ($\mu\text{mol g}^{-1}$)	S ($\mu\text{mol g}^{-1}$)	S+G ($\mu\text{mol g}^{-1}$)	S/G
<i>knat3</i>	24.6 \pm 0.36***	10.4 \pm 0.56***	35 \pm 0.78***	0.42 \pm 0.021
<i>knat7</i>	49.3 \pm 0.45***	14.2 \pm 0.79*	63.48 \pm 1.24***	0.29 \pm 0.014***
<i>knat3 knat7</i>	46.8 \pm 1.04***	3.2 \pm 0.26***	50 \pm 0.92	0.07 \pm 0.006***
WT	36.7 \pm 0.81	16.2 \pm 0.70	52.9 \pm 1.37	0.44 \pm 0.015

Data are mean \pm SD, including three replicates. Eight-week-old main stem of *Arabidopsis* was selected to determine lignin monomer content. Significant differences from WT are shown: *P<0.05, ***P<0.001, Student's *t*-test. G, guaiacyl lignin; S, syringyl lignin.

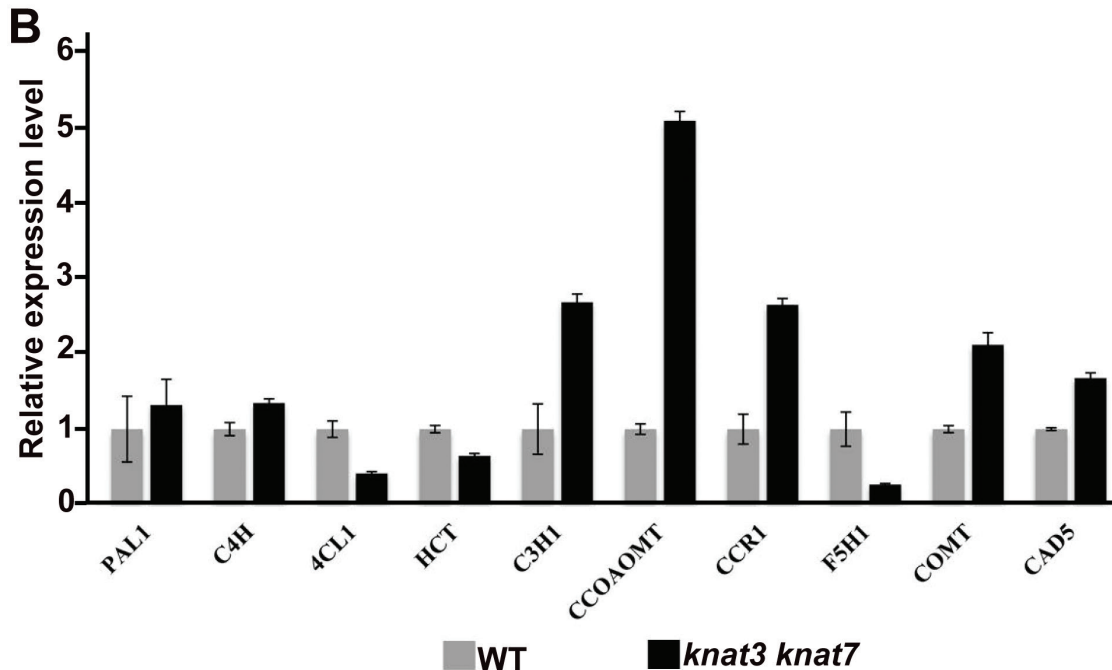
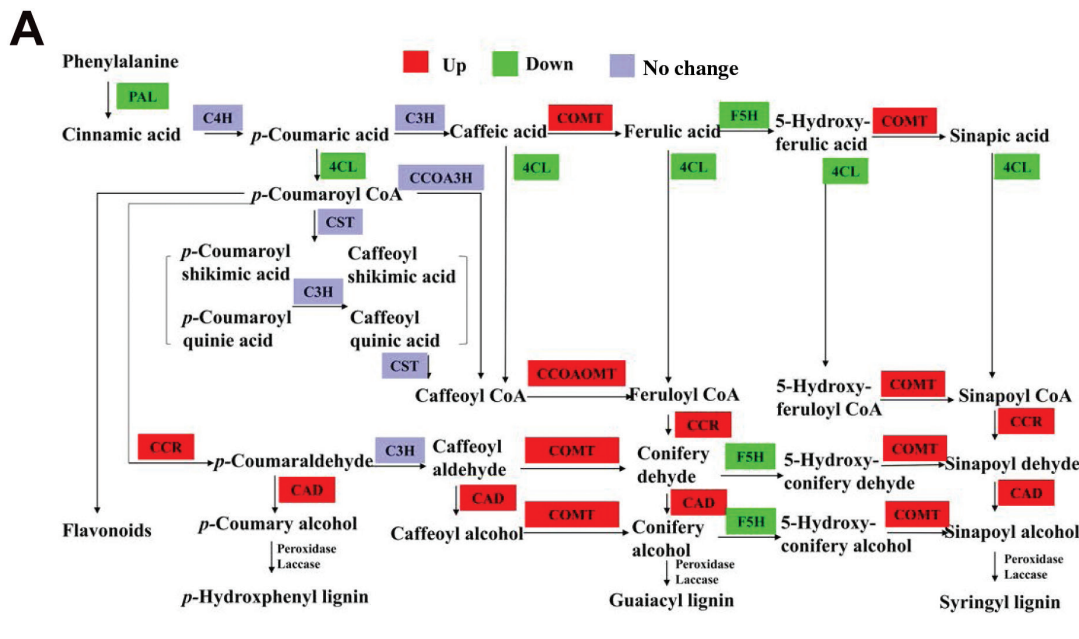


Fig. 5. S-lignin synthesis gene *F5H* was down-regulated. (A) RNA-seq data showing the expression changes of lignin pathway gene. The results were based on the difference of multiple fold change ≥ 2 and the error rate FDR < 0.01 as the screening criteria. (B) qRT-PCR was used to detect the relative expression of lignin metabolic pathway genes between WT and *knat3 knat7* mutant. PAL, Phenylalanine Ammonia Lyase; C4H, Cinnamate 4-Hydroxylase; 4CL, 4-Coumarate CoA Ligase; C3H, Coumaroyl Shikimate 3'-Hydroxylase; CAD, Cinnamyl Alcohol Dehydrogenase; F5H, Ferulate 5-Hydroxylase. The expression level of each gene in the WT was assigned a value of 1 and *EF1 α* was used as an internal reference. The data represent the mean and SD of three biological repetitions and four technical repetitions. (This figure is available in color at JXB online.)

KNAT3 has a main effect in regulating the expression of *F5H* gene

Because the significant decrease of S-lignin in *knat3 knat7* might be caused by the down-regulation of *F5H* expression, we explored whether KNAT3 and KNAT7 can regulate the expression of the *F5H* gene. The 2171 bp upstream region of the *F5H* gene was cloned and inserted into a reporter vector harboring the luciferase gene (*LUC*). p35S:KNAT3 and p35S:KNAT7 were constructed as effectors (Fig. 6A), and transiently transformed into Arabidopsis protoplast cells. The results showed that both KNAT3 and KNAT7 can activate *LUC* expression, that KNAT3 had higher activity than KNAT7, and that the KNAT3+KNAT7 combination showed the highest activation (Fig. 6B). These results indicate that KNAT3 and KNAT7 can work on the *F5H* promoter to regulate *LUC* expression.

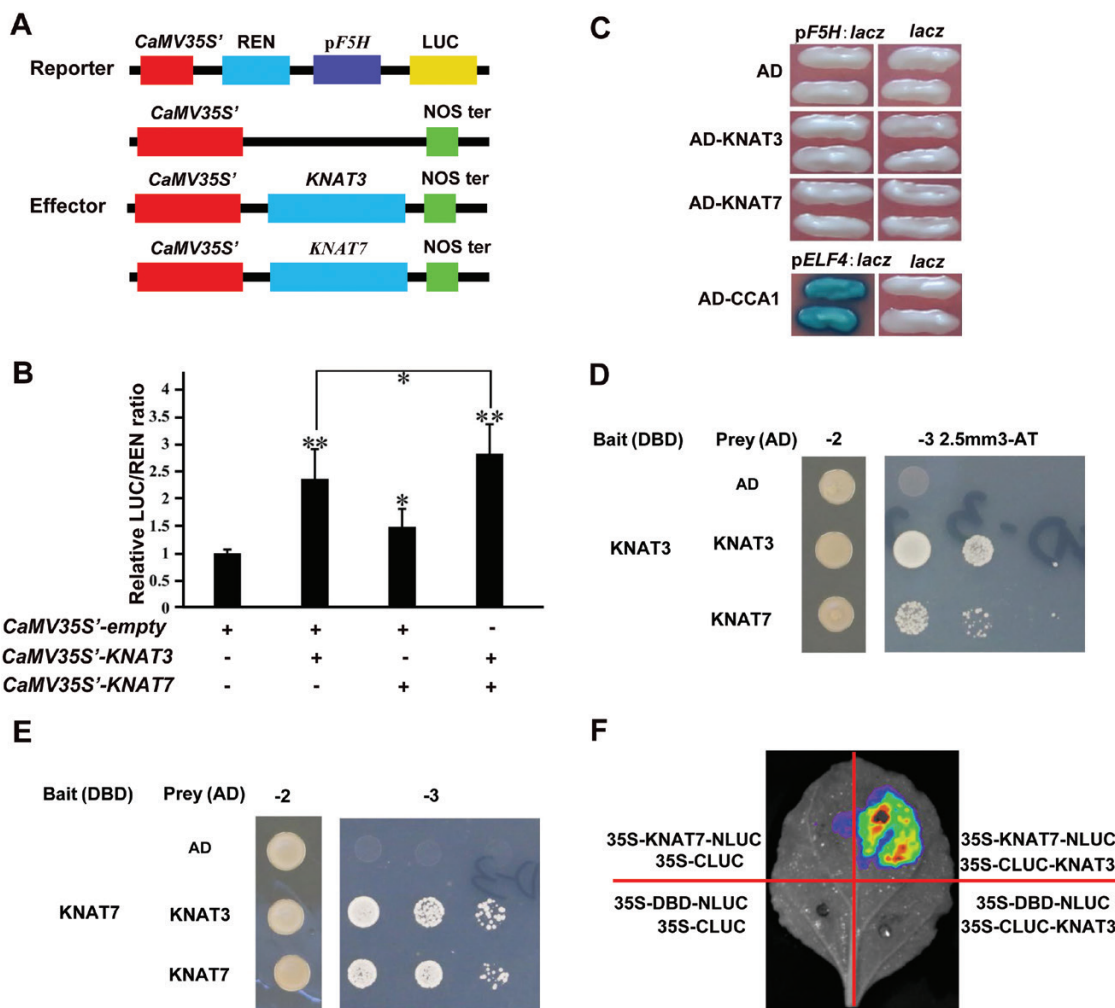


Fig. 6. KNAT3 and KNAT7 can form a dimer to activate *F5H* expression. (A) Schematic representation of the transcriptional activation reporter and effector system. (B) The activation was carried out by adding different reporters and effectors to the Arabidopsis protoplasts. The ratio of LUC and REN in the CaMV35S'-empty cells with only reporters was used as control and assigned a value of 1. Column height indicates the mean \pm SD of the relative LUC/REN ratio with three biological replicates; $n=4$. * $P<0.05$, ** $P<0.01$, Student's *t*-test. (C) Yeast one-hybrid assay detects KNAT3 and KNAT7 binding with the *F5H* promoter. Positive binding showed as blue after X-gal was added. As a negative control (AD), KNAT3 and KNAT7 cannot directly bind to the *F5H* promoter. (D, E) Interaction of KNAT3 and KNAT7 proteins was examined in yeast cells, with KNAT3 CDS and GAL4 DNA-binding region (DBD) fused as a bait protein, and GAL4 transcriptional activation region (AD) fused with KNAT3 or KNAT7 protein used as prey (D), or the opposite of bait and prey (E). After transformation, the yeast was spotted on SD-Leu-Trp (-2) medium and SD-Leu-Trp-His (-3) screening medium containing 2.5 mm 3-aminotriazole, and AD was used as a negative control. KNAT7 and KNAT3 can form homodimers and heterodimers. (F) KNAT3 and KNAT7 interact in plants, and the four quadrants show different transformation combinations. Only the mixture of KNAT3 and KNAT7 proteins by split luciferase complementation shows fluorescence. (This figure is available in color at JXB online.)

In order to detect whether KNAT3 and KNAT7 can directly or indirectly activate the *F5H* gene, a yeast one-hybrid system was used to check the binding effects. Unexpectedly, neither KNAT3 nor KNAT7 bound directly to the *F5H* promoter region (Fig. 6C). Therefore, we hypothesized that KNAT3 and KNAT7 might activate other genes or form a protein complex to regulate the expression of *F5H*. Up until now there are no proteins reported to directly regulate *F5H* in Arabidopsis, so we speculated that the regulation of *F5H* may be accomplished by a larger complex.

KNOXs, as members of the TALE homeodomain superfamily (Hake *et al.*, 2004; Hay and Tsiantis, 2010), have the potential to form homo- or heterodimers. We found that KNAT3 and KNAT7 can form homodimers and a heterodimer in a yeast two-hybrid assay (Fig. 6D, E), as reported by Hackbusch

et al. (2005). Split luciferase complementation experiments verified that KNAT3 and KNAT7 form dimers *in planta* as well (Fig. 6F). When KNAT3 and KNAT7 were introduced simultaneously into the Arabidopsis protoplast cells, we found that the mixture of KNAT3 and KNAT7 showed a stronger activation effect than KNAT3 alone (Fig. 6B), suggesting that the heterodimer might be more effective than the homodimers.

KNAT3 but not KNAT7 interacts with NST1 and NST2 to regulate the expression of F5H

Since neither KNAT3 nor KNAT7 directly binds to the *F5H* promoter but showed weak activation of *F5H* expression, we deduced that some proteins or factors in the regulation system had been missed. Hence, we used KNAT3 as a bait protein

to screen an *Arabidopsis* transcription factor library by yeast two-hybrid screening (Mitsuda *et al.*, 2010). *NST1* and *NST2* were identified in screening, and these have been regarded as the top-level switches to regulate secondary cell wall formation (Mitsuda *et al.*, 2005, 2006; Zhong *et al.*, 2010; Zhou *et al.*, 2014; Zhong and Ye, 2015). We further verified the interactions between KNAT3/7 and *NST1*, *NST2*, and *SND1* (also named as *NST3*) by yeast two-hybrid, split-luciferase complementation, co-immunoprecipitation, and immunoblot analyses (Fig. 7A–E). The results showed that only KNAT3, but not KNAT7, interacted with *NST1* and *NST2*. Neither KNAT3 nor KNAT7 can interact with *SND1* (Fig. 7A–E).

Furthermore, we investigated whether the heterologous complex formed by KNAT3 and *NST1/NST2* activates *F5H* expression. We performed a transcriptional activation

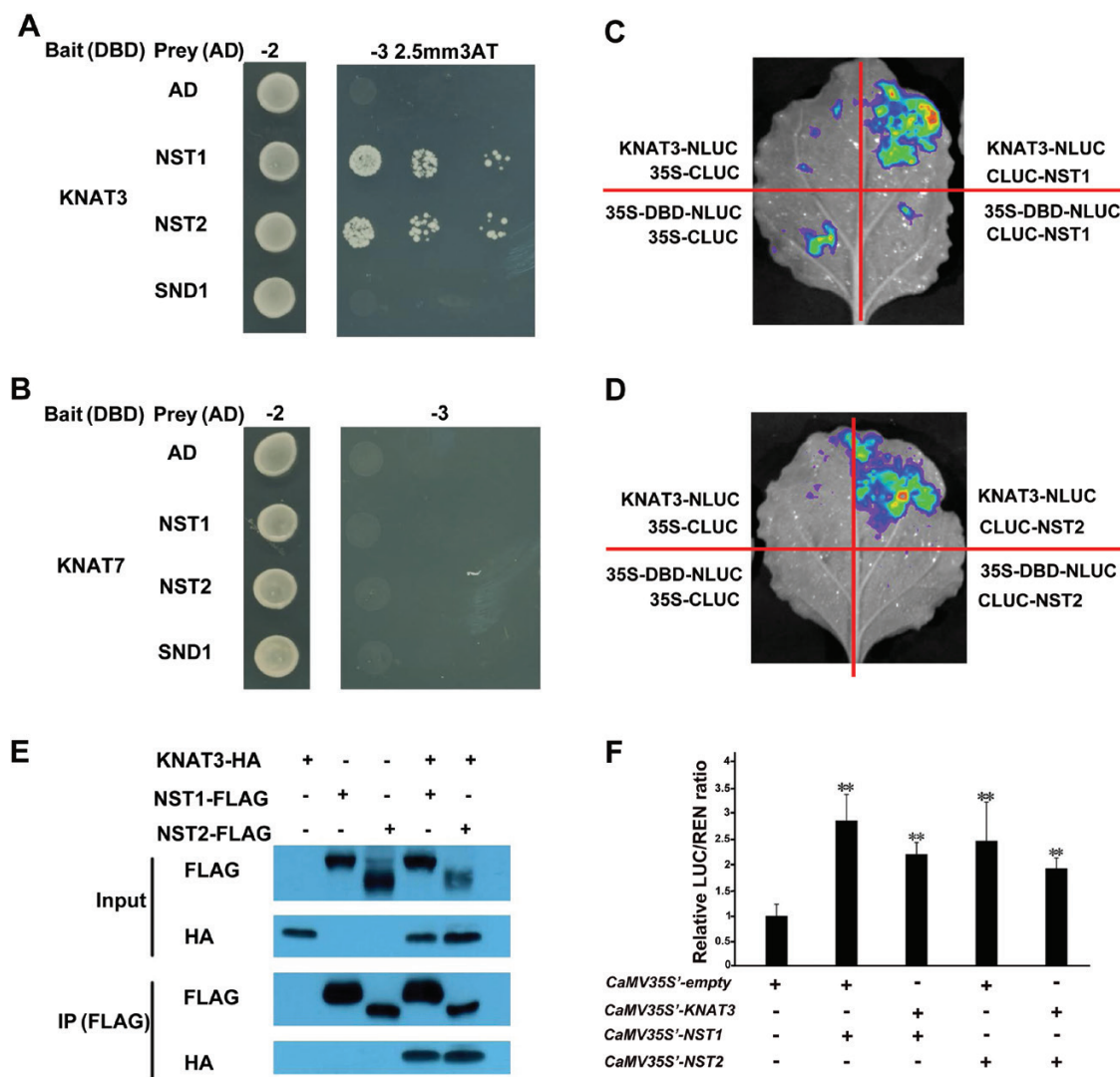


Fig. 7. KNAT3/7 interact with *NST1/NST2* proteins. (A) KNAT3 and *NST1/NST2* proteins interact by yeast two-hybrid assay, with KNAT3 CDS and GAL4 DNA-binding region (DBD) fusion as bait protein and GAL4 transcriptional activation region (AD) fused with *NST1/NST2/SND1* protein as prey. The transformed yeast was spotted in SD-Leu-Trp (-2) medium and SD-Leu-Trp-His (-3) with 2.5 mm 3-aminotriazole, and AD was used as a negative control. (B) KNAT7 cannot interact with *NST1/NST2/SND1* in yeast cells. (C, D) KNAT3 and *NST1/NST2* interact in plants. The four quadrants show different combinations of transformation constructs. (E) Co-immunoprecipitation assay of KNAT3-HA and *NST1/2*-FLAG. The proteins were immunoprecipitated with anti-FLAG antibody and then probed with anti-HA antibody. (F) Transcriptional activation experiments in which reporters tested different effectors in *Arabidopsis* protoplasts. CaMV35S'-empty with only reporter was used as control with the ratio of LUC and REN assigned a value of 1 for normalization. Data are mean \pm SD of the relative LUC/REN ratio of each combination with three biological replicates; $n=4$. ** $P<0.01$, Student's *t*-test. (This figure is available in color at JXB online.)

experiment in Arabidopsis protoplasts. The results revealed that NST1 and NST2 alone could weakly activate the *F5H* promoter, and no further activation was gained after KNAT3 was added (Fig. 7F). This indicates that some factors in the regulation of *F5H* expression might still be missing and further exploration is required.

Discussion

There are four members of Arabidopsis KNOX class II genes, among which *KNAT3*, *KNAT4*, and *KNAT5* play a functionally redundant role in regulating leaf morphology, and the serrated leaf phenotypes *knat3*, *knat3 knat5*, and *knat3 knat4 knat5* show a gradual progression (Furumizu *et al.*, 2015). However, the effects of *KNAT3*, *KNAT4*, and *KNAT5* on secondary wall formation have not been reported. *KNAT7*, also called *IRX11*, has been reported to be linked with vessel cell development as its mutant showed inwardly collapsed vessel cells forming irregular xylem (Brown *et al.*, 2005). Some reports revealed that *KNAT7* acts as a transcriptional repressor to inhibit secondary cell wall deposition (Li *et al.*, 2011, 2012), but the *knat7* mutant showed thinner vessel cells despite thicker interfascicular fiber cells (Li *et al.*, 2012). *KNAT7* can also act as a transcriptional activator to activate the expression of xylan synthesis genes (He *et al.*, 2018). To better explain this contradiction, we further combined other KNOX II members with *KNAT7* in this study. We found that *KNAT3* and *KNAT7* had obvious functional redundancy in regulating the synthesis of Arabidopsis secondary cell walls. Coincidentally, Wang *et al.*, 2020a recently reported *KNAT3* and *KNAT7* work cooperatively to influence secondary cell wall deposition. Their work was mainly focused on the functions of *KNAT3* and *KNAT7* in secondary cell wall synthesis, including hemicellulose and lignin synthesis. They used phenotypic and chemical analysis results and their conclusions are in close agreement with ours. In the present study, we focused on lignin, especially the S-lignin subunit, and we explained the reason why the S-subunit lignin decreases in mutants by protein interaction and pathway analysis.

Dominant repressor plants p35S:KNAT3-SRDX and p35S:KNAT7-SRDX displayed severe defects in stem development and both showed similar dwarf phenotypes (see Supplementary Fig.S1) indicating that these genes exhibit functional redundancy. The expression patterns demonstrated that *KNAT3* and *KNAT7* were co-expressed in secondary xylem and interfascicular fiber tissues (Fig. 1). The loss-of-function *knat3 knat7* double mutant showed significantly reduced height at 6 weeks of age (Fig. 2D, E), which is consistent with *KNAT3* and *KNAT7* dominant repressor plants. In addition to irregular xylem, the *knat7* mutant showed a thicker interfascicular fiber wall, thinner xylem vessel wall, and increased lignin content (Li *et al.*, 2011; He *et al.*, 2018). In the literature there are reports that *KNAT7* interacts with MYB75, BLH6, and OFP4, forming a complex to inhibit secondary cell wall formation (Hackbusch *et al.*, 2005; Bhargava *et al.*, 2010; Li *et al.*, 2011; Liu *et al.*, 2014), which indicates that *KNAT7* has complicated and spatiotemporally differentiated functions based on specific

cell type, tissue, and interacting regulators. *knat3* differs from *knat7* in that it does not have an irregular xylem phenotype but has a thinner secondary cell wall of the interfascicular fiber cells. However, *knat3 knat7* has an enhanced *irx* phenotype (Fig. 3) and significantly reduced cell wall thickness in vessels, xylary and interfascicular fibers as compared with *knat7*. This phenotype indicated that *KNAT3*, as a homolog of *KNAT7*, has functional redundancy in the development of secondary cell wall, and *KNAT3* is a transcriptional activator of secondary wall thickening. We found *KNAT3* and *KNAT7* proteins can form heterodimers in the yeast two-hybrid assay and that only *KNAT3* interacts with *NST1* and *NST2*, the two main regulators involved in regulation of secondary cell wall thickening (Mitsuda *et al.*, 2005; Zhong and Ye, 2015). Based on these results, we propose a working model of *KNAT3* and *KNAT7* as shown in Fig. 8. *KNAT3* interacts with *NST1/2*, the positive regulators of the secondary cell wall, but *KNAT7* interacts with *MYB75/BLH6/OFP4*, the negative regulators of the secondary cell wall. Interestingly, secondary cell wall thickness in interfascicular fibers was reduced in the *nst1 nst3* double mutant (Zhong *et al.*, 2007; Zhong and Ye, 2015) meaning that *NST1* can specifically function in this region. Thus, we speculate that, in the *knat7* mutant, a *KNAT3*–*NST1* complex stimulates downstream genes to promote cell wall synthesis in interfascicular fibers and produces thicker interfascicular fiber wall. At the same time, *NST1* is a fiber-specific transcription factor and *KNAT3* interacts with *NST1* there. S-lignin is predominantly deposited in fiber regions, so the *knat3* mutant showed a lower fiber cell wall thickness (Fig. 3F, G) and less S-lignin (Table 1).

In dicots, lignin is mainly composed of S- and G-lignin sub-units with a very low concentration of H-lignin (Vogel, 2008). Acid-soluble lignin was preferentially derived from the condensed syringyl lignin while the guaiacyl lignin was insoluble in 72% sulfuric acid (Yue *et al.*, 2012). It is possible that acid-soluble lignin has a relatively high S-lignin content, and acid-insoluble lignin has a high G-lignin content (Fig. 4A). Thus, the lower acid-insoluble lignin might result from the lower content of S-lignin in *knat3* and *knat3 knat7*, as compared with *knat7* and WT (Fig. 4A; Table 1). Some reports suggest that *KNAT7* is a negative regulator of lignin biosynthesis and the loss-function mutant of *knat7* had increased lignin content

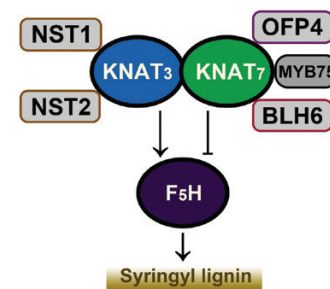


Fig. 8. Hypothetical model of *KNAT3/KNAT7* synergistical regulation of S-lignin biosynthesis. *KNAT3* and *KNAT7* can form a heterodimer. The proteins *MYB75*, *OFP4*, and *BLH6* were reported as negative regulators interacting with *KNAT7* to repress *F5H* in some cell types and the proteins *NST1/2* were reported as positive regulators interacting with *KNAT3* to activate *F5H* in specific cells. (This figure is available in color at JXB online.)

(Brown *et al.*, 2005; Li *et al.*, 2011). Our determination of lignin content evidenced that the increase of total lignin content in *knat7* was due to a large increase of G-lignin with concomitant slight decrease of S-lignin. The contents of G-, S- and total lignin in *knat3* were significantly reduced, but the lignin S/G ratio remained unchanged, indicating KNAT3 positively regulates lignin biosynthesis. Although the total lignin in *knat3 knat7* remained unchanged, the S-lignin was greatly reduced and the G-lignin was increased, eventually resulting in an 84% reduction of the S/G ratio (Fig. 4; Table 1). Therefore, we believe that KNAT3 synergizes with KNAT7 in lignin synthesis, and KNAT3 plays a dominant role in controlling S-lignin synthesis.

In the lignin synthesis pathway, F5H is a key enzyme responsible for hydroxylation of G-lignin monomer to form S-lignin (Humphreys *et al.*, 1999; Osakabe *et al.*, 1999; Franke *et al.*, 2000; García *et al.*, 2014). Our transcriptomic data of *knat3 knat7* indicated that the differentially expressed genes were significantly enriched in the phenylalanine metabolic pathway (see Supplementary Fig. S4) and most of the gene expression was up-regulated, while the expression of 4CL and *F5H* was down-regulated (Fig. 5). Therefore, the down-regulation of *F5H* could contribute to the increased G-lignin in *knat7* mutant with unchanged total lignin content in most mutants. This is also a good explanation for the increase in G-lignin content and the large reduction of S-lignin in *knat3 knat7*. We also checked the profiles of all MYB transcription factors in our transcriptome data. We found that *MYB20*, *MYB69*, and *MYB86* were down-regulated, but both *MYB46* and *MYB83*, regarded as activators of secondary wall biosynthesis, and *MYB75*, *MYB4* and *MYB7*, regarded as repressors of secondary wall biosynthesis, were up-regulated (Supplementary Table S2; McCarthy *et al.*, 2009; Bhargava *et al.*, 2010; Ko *et al.*, 2014; Wang *et al.*, 2020b). Thus, KNAT3 and KNAT7 might have a complicated regulatory network or feedback network. Because the *myb103* mutant can also decrease *F5H* gene expression (Öhman *et al.*, 2013), it is unclear whether MYB103 works upstream or downstream of KNAT3/KNAT7 in regulating *F5H* gene expression. According to our transcriptome and qPCR analysis, the *MYB103* expression level showed no obvious difference in the *knat3 knat7* double mutant, compared with the WT (Supplementary Table S2; Supplementary Fig. S5A, B), and the expression levels of KNAT3 and KNAT7 increased in the *myb103* mutant (Supplementary Fig. S5B). The increased KNAT7 expression is especially obvious. The cause of increased KNAT3/7 expression might be due to compensation. All the results indicate that MYB103 and KNAT3/KNAT7 might function in independent pathways to regulate *F5H* expression.

Transcriptional activation experiments in Arabidopsis protoplasts revealed that both KNAT3 and KNAT7 weakly activated the *F5H* promoter, suggesting that KNAT3 and KNAT7 indirectly regulate *F5H* (Fig. 6). It is known that MYB58 and MYB63 directly activate the expression of lignin synthetic genes by binding to the AC element or degenerated AC element of the promoter regions of those genes (Zhou *et al.*, 2009; Zhao and Dixon, 2011). However, there is no AC element in the *F5H* promoter region, except that NST1 and

SND1 were reported to bind directly to the *F5H* promoter region to activate *F5H* expression in *Medicago truncatula* (Zhao *et al.*, 2010). Arabidopsis SND1 cannot directly activate *F5H* expression (Öhman *et al.*, 2013). Our yeast one-hybrid experiments showed that neither KNAT3 nor KNAT7 could directly bind to the promoter of *F5H*. Only KNAT3, not KNAT7, interacts with the top secondary cell wall regulatory factors NST1/NST2. Although NST1 and NST2 can weakly activate *F5H* expression, some effectors in the regulatory cascade or complex may still be missing (Fig. 7). The *F5H* regulation mechanism remains to be further explored.

As we know, fibers are enriched in S-lignin, whereas guaiacyl-enriched lignin is mainly deposited in vessels (Fergus and Goring, 1970a, b; Masha and Goring, 1975; Saka and Goring, 1985). Furthermore, the deposition of S-lignin precedes that of G-lignin in interfascicular fiber elements (Terashima *et al.*, 1986; Saka and Goring, 1988). NST1 and NST2 are fiber-specific transcription factors, which interact with KNAT3, and this could be the reason for S-lignin biosynthesis via activation of *F5H* in the fiber. Although the *knat3 knat7* mutant has collapsed vessels as with the *knat7* mutant, both mutants contain increased G-lignin content, and the expression of G-lignin pathway genes, such as *CCoAOMT*, is up-regulated as well. To investigate the cause of the increase in G-lignin, the expression of VASCULAR-RELATED NAC-DOMAIN 6 (VND6) and 7 (VND7), which work as master regulators of metaxylem and protoxylem vessel cell fates, respectively (Kubo *et al.*, 2005; Ohashi-Ito *et al.*, 2010), was examined in the transcriptome analysis. The result showed that the expression of *VND6* and *VND7* only slightly decreased in the *knat3 knat7* mutant in comparison with WT (see Supplementary Fig S5A). Additionally, we did not detect interactions between KNAT7 and VND6/7 by yeast-two hybrid assay (data not shown). Thus, we deduce that the increasing G-lignin content in *knat3 knat7* might be due to the increase of some G-lignin biosynthesis-related genes and down-regulation of *F5H*.

This study demonstrates that KNAT3 and KNAT7 play a synergistic role in regulating the growth and development of Arabidopsis secondary cell wall. The KNAT3 mutant enhances the phenotype of *knat7* in the secondary cell wall of xylem vessels (Figs 3, 4). In addition, KNAT3 interacts with NST1/NST2 to promote expression of *F5H* to regulate the synthesis of S-lignin. In the synthesis of secondary cell walls including lignin, interactions such as KNAT7 and BLH6/MYB75/OFP4 may function as transcriptional repressors. On the other hand, KNAT3 synergizing with KNAT7 functions positively for the synthesis of S-lignin (Fig. 8). This study complements the transcriptional regulatory network of secondary cell walls and clarifies the regulation of S-lignin by KNAT3 and KNAT7.

Supplementary data

Supplementary data are available at JXB online.

Fig. S1. Chimeric repressors in KNAT3 and KNAT7.

Fig. S2. Mäule staining of cross-section of stem in dominant repressor transgenic plants.

Fig. S3. Mäule staining of cross-section of stem of *knat3 knat7* complementary plants.

Fig. S4. Pathway enrichment analysis of WT and *knat3 knat7* RNA-seq.

Fig. S5. Expression levels of *KNAT3* and *KNAT7* in *myb103* mutant.

Table S1. Primer sequences used in this study.

Table S2. RNA-seq analysis of MYB differentially expressed genes (WT versus *knat3 knat7*)

Acknowledgements

We thank the Arabidopsis Biological Resource Center for seeds of the T-DNA insertion mutant. Financial support for this work was obtained the National Natural Science Foundation of China (Grant Numbers 31870653, 31670670, 31811530009).

Author contributions

A-MW and WQ designed the study and wrote the manuscript. WQ, QY, XZ, JC, FY, JH, LY, and LL, performed the experiments. FL, NM, and MO-T helped with the techniques and analysed the data.

Conflict of interest

The authors have no conflicts of interest to declare.

Data availability

All relevant data can be found within the manuscript and its supporting materials.

References

- Bhargava A, Mansfield SD, Hall HC, Douglas CJ, Ellis BE.** 2010. MYB75 functions in regulation of secondary cell wall formation in the *Arabidopsis* inflorescence stem. *Plant Physiology* **154**, 1428–1438.
- Boerjan W, Ralph J, Baucher M.** 2003. Lignin biosynthesis. *Annual Review of Plant Biology* **54**, 519–546.
- Bonawitz ND, Chapple C.** 2010. The genetics of lignin biosynthesis: connecting genotype to phenotype. *Annual Review of Genetics* **44**, 337–363.
- Brown DM, Zeef LA, Ellis J, Goodacre R, Turner SR.** 2005. Identification of novel genes in *Arabidopsis* involved in secondary cell wall formation using expression profiling and reverse genetics. *The Plant Cell* **17**, 2281–2295.
- Clough SJ, Bent AF.** 1998. Floral dip: a simplified method for *Agrobacterium*-mediated transformation of *Arabidopsis thaliana*. *The Plant Journal* **16**, 735–743.
- Cosgrove DJ, Jarvis MC.** 2012. Comparative structure and biomechanics of plant primary and secondary cell walls. *Frontiers in Plant Science* **3**, 204.
- Fergus BJ, Goring DAI.** 1970a. The location of guaiacyl and syringyl lignins in birch xylem tissue. *Holzforschung* **24**, 113–117.
- Fergus BJ, Goring DAI** 1970b. The distribution of lignin in birch wood as determined by ultraviolet microscopy. *Holzforschung* **24**, 118–124.
- Franke R, McMichael CM, Meyer K, Shirley AM, Cusumano JC, Chapple C.** 2000. Modified lignin in tobacco and poplar plants over-expressing the *Arabidopsis* gene encoding ferulate 5-hydroxylase. *The Plant Journal* **22**, 223–234.
- Furumizu C, Alvarez JP, Sakakibara K, Bowman JL.** 2015. Antagonistic roles for KNOX1 and KNOX2 genes in patterning the land plant body plan following an ancient gene duplication. *PLoS Genetics* **11**, e1004980.
- García JR, Anderson N, Le-Feuvre R, Iturra C, Elissetche J, Chapple C, Valenzuela S.** 2014. Rescue of syringyl lignin and sinapate ester biosynthesis in *Arabidopsis thaliana* by a coniferaldehyde 5-hydroxylase from *Eucalyptus globulus*. *Plant Cell Reports* **33**, 1263–1274.
- Goicoechea M, Lacombe E, Legay S, et al.** 2005. EgMYB2, a new transcriptional activator from *Eucalyptus xylem*, regulates secondary cell wall formation and lignin biosynthesis. *The Plant Journal* **43**, 553–567.
- Hackbusch J, Richter K, Müller J, Salamini F, Uhrig JF.** 2005. A central role of *Arabidopsis thaliana* ovate family proteins in networking and subcellular localization of 3-aa loop extension homeodomain proteins. *Proceedings of the National Academy of Sciences, USA* **102**, 4908–4912.
- Hake S, Smith HM, Holtan H, Magnani E, Mele G, Ramirez J.** 2004. The role of knox genes in plant development. *Annual Review of Cell and Developmental Biology* **20**, 125–151.
- Han X, Yu H, Yuan R, Yang Y, An F, Qin G.** 2019. Arabidopsis transcription factor TCP5 controls plant thermomorphogenesis by positively regulating PIF4 activity. *iScience* **15**, 611–622.
- Hay A, Tsiantis M.** 2010. KNOX genes: versatile regulators of plant development and diversity. *Development* **137**, 3153–3165.
- He JB, Zhao XH, Du PZ, Zeng W, Beahan CT, Wang YQ, Li HL, Bacic A, Wu AM.** 2018. KNAT7 positively regulates xylan biosynthesis by directly activating *IRX9* expression in *Arabidopsis*. *Journal of Integrative Plant Biology* **60**, 514–528.
- Hellens RP, Allan AC, Friel EN, Bolitho K, Grafton K, Templeton MD, Karunairetnam S, Gleave AP, Laing WA.** 2005. Transient expression vectors for functional genomics, quantification of promoter activity and RNA silencing in plants. *Plant Methods* **1**, 13.
- Hiratsu K, Matsui K, Koyama T, Ohme-Takagi M.** 2003. Dominant repression of target genes by chimeric repressors that include the EAR motif, a repression domain, in *Arabidopsis*. *The Plant Journal* **34**, 733–739.
- Hiratsu K, Mitsuda N, Matsui K, Ohme-Takagi M.** 2004. Identification of the minimal repression domain of SUPERMAN shows that the DLELRL hexapeptide is both necessary and sufficient for repression of transcription in *Arabidopsis*. *Biochemical and Biophysical Research Communications* **321**, 172–178.
- Humphreys JM, Hemm MR, Chapple C.** 1999. New routes for lignin biosynthesis defined by biochemical characterization of recombinant ferulate 5-hydroxylase, a multifunctional cytochrome P450-dependent monooxygenase. *Proceedings of the National Academy of Sciences, USA* **96**, 10045–10050.
- Jefferson RA, Kavanagh TA, Bevan MW.** 1987. GUS fusions: beta-glucuronidase as a sensitive and versatile gene fusion marker in higher plants. *The EMBO Journal* **6**, 3901–3907.
- Kerstetter R, Vollbrecht E, Lowe B, Veit B, Yamaguchi J, Hake S.** 1994. Sequence analysis and expression patterns divide the maize *knotted1-like* homeobox genes into two classes. *The Plant Cell* **6**, 1877–1887.
- Kim H, Ralph J.** 2010. Solution-state 2D NMR of ball-milled plant cell wall gels in DMSO-d₆/pyridine-d₅. *Organic & Biomolecular Chemistry* **8**, 576–591.
- Ko JH, Jeon HW, Kim WC, Kim JY, Han KH.** 2014. The MYB46/MYB83-mediated transcriptional regulatory programme is a gatekeeper of secondary wall biosynthesis. *Annals of Botany* **114**, 1099–1107.
- Kubo M, Udagawa M, Nishikubo N, Horiguchi G, Yamaguchi M, Ito J, Mimura T, Fukuda H, Demura T.** 2005. Transcription switches for protoxylem and metaxylem vessel formation. *Genes & Development* **19**, 1855–1860.
- Lacombe E, Van Doorslaer J, Boerjan W, Bouquet AM, Grima-Pettenati J.** 2000. Characterization of cis-elements required for vascular expression of the *Cinnamoyl CoA Reductase* gene and for protein–DNA complex formation. *The Plant Journal* **23**, 663–676.
- Li E, Bhargava A, Qiang W, Friedmann MC, Forneris N, Savidge RA, Johnson LA, Mansfield SD, Ellis BE, Douglas CJ.** 2012. The Class II KNOX gene *KNAT7* negatively regulates secondary wall formation in *Arabidopsis* and is functionally conserved in *Populus*. *New Phytologist* **194**, 102–115.
- Li E, Wang S, Liu Y, Chen JG, Douglas CJ.** 2011. OVATE FAMILY PROTEIN4 (OFP4) interaction with KNAT7 regulates secondary cell wall formation in *Arabidopsis thaliana*. *The Plant Journal* **67**, 328–341.
- Liu Y, You S, Taylor-Teeple M, Li WL, Schuetz M, Brady SM, Douglas CJ.** 2014. BEL1-LIKE HOMEO DOMAIN6 and KNOTTED

- ARABIDOPSIS THALIANA7 interact and regulate secondary cell wall formation via repression of REVOLUTA. *The Plant Cell* **26**, 4843–4861.
- Mansfield SD, Kim H, Lu F, Ralph J.** 2012. Whole plant cell wall characterization using solution-state 2D NMR. *Nature Protocols* **7**, 1579–1589.
- McCarthy RL, Zhong R, Ye ZH.** 2009. MYB83 is a direct target of SND1 and acts redundantly with MYB46 in the regulation of secondary cell wall biosynthesis in *Arabidopsis*. *Plant & Cell Physiology* **50**, 1950–1964.
- Mitsuda N, Hiratsu K, Todaka D, Nakashima K, Yamaguchi-Shinozaki K, Ohme-Takagi M.** 2006. Efficient production of male and female sterile plants by expression of a chimeric repressor in *Arabidopsis* and rice. *Plant Biotechnology Journal* **4**, 325–332.
- Mitsuda N, Ikeda M, Takada S, Takiguchi Y, Kondou Y, Yoshizumi T, Fujita M, Shinozaki K, Matsui M, Ohme-Takagi M.** 2010. Efficient yeast one-/two-hybrid screening using a library composed only of transcription factors in *Arabidopsis thaliana*. *Plant & Cell Physiology* **51**, 2145–2151.
- Mitsuda N, Seki M, Shinozaki K, Ohme-Takagi M.** 2005. The NAC transcription factors NST1 and NST2 of *Arabidopsis* regulate secondary wall thickenings and are required for anther dehiscence. *The Plant Cell* **17**, 2993–3006.
- Mukherjee K, Brocchieri L, Bürglin TR.** 2009. A comprehensive classification and evolutionary analysis of plant homeobox genes. *Molecular Biology and Evolution* **26**, 2775–2794.
- Musha Y, Goring DAI** 1975. Distribution of syringyl and guaiacyl moieties in hardwoods as indicated by ultraviolet microscopy. *Wood Science and Technology* **9**, 45–58.
- Nakagawa T, Suzuki T, Murata S, et al.** 2007. Improved Gateway binary vectors: high-performance vectors for creation of fusion constructs in transgenic analysis of plants. *Bioscience, Biotechnology, and Biochemistry* **71**, 2095–2100.
- Ohashi-Ito K, Oda Y, Fukuda H.** 2010. *Arabidopsis* VASCULAR-RELATED NAC-DOMAIN6 directly regulates the genes that govern programmed cell death and secondary wall formation during xylem differentiation. *The Plant Cell* **22**, 3461–3473.
- Öhman D, Demedts B, Kumar M, Gerber L, Gorzsás A, Goeminne G, Hedenstrom M, Ellis B, Boerjan W, Sundberg B.** 2013. MYB103 is required for FERULATE-5-HYDROXYLASE expression and syringyl lignin biosynthesis in *Arabidopsis* stems. *The Plant Journal* **73**, 63–76.
- Osakabe K, Tsao CC, Li L, Popko JL, Umezawa T, Carraway DT, Smeltzer RH, Joshi CP, Chiang VL.** 1999. Coniferyl aldehyde 5-hydroxylation and methylation direct syringyl lignin biosynthesis in angiosperms. *Proceedings of the National Academy of Sciences, USA* **96**, 8955–8960.
- Patzlaff A, McInnis S, Courtenay A, et al.** 2003. Characterisation of a pine MYB that regulates lignification. *The Plant Journal* **36**, 743–754.
- Pradhan MP, Loque D.** 2014. Histochemical staining of *Arabidopsis thaliana* secondary cell wall elements. *Journal Visualized Experiments* (87), 51381.
- Saka S, Goring DAI.** 1985. Localization of lignin in wood cell walls. In: Higuchi T, ed. *Biosynthesis and biodegradation of wood components*. New York: Academic Press, 141–160.
- Saka S, Goring DAI.** 1988. The distribution of lignin in white birch wood as determined by bromination with TEM-EDXA. *Holzforschung* **42**, 149–153.
- Tao Q, Guo D, Wei B, et al.** 2013. The TIE1 transcriptional repressor links TCP transcription factors with TOPLESS/TOPLESS-RELATED corepressors and modulates leaf development in *Arabidopsis*. *The Plant Cell* **25**, 421–437.
- Terashima N, Fukushima K, Takabe K.** 1986. Heterogeneity in formation of lignin: An autoradiographic study on the formation of guaiacyl and syringyl lignin in *Magnolia kobus*. *Holzforschung* **42**, 101–105.
- Vanholme R, Cesarino I, Rataj K, et al.** 2013. Caffeoyl shikimate esterase (CSE) is an enzyme in the lignin biosynthetic pathway in *Arabidopsis*. *Science* **341**, 1103–1106.
- Vogel J.** 2008. Unique aspects of the grass cell wall. *Current Opinion in Plant Biology* **11**, 301–307.
- Wang KL, Wang B, Hu R, Zhao X, Li H, Zhou G, Song L, Wu AM.** 2019. Characterization of hemicelluloses in *Phyllostachys edulis* (moso bamboo) culm during xylogenesis. *Carbohydrate Polymers* **221**, 127–136.
- Wang S, Yamaguchi M, Grienberger E, Martone PT, Samuels AL, Mansfield SD.** 2020a. The Class II KNOX genes KNAT3 and KNAT7 work cooperatively to influence secondary cell wall deposition and provide mechanical support to *Arabidopsis* stems. *The Plant Journal* **101**, 293–309.
- Wang XC, Wu J, Guan ML, Zhao CH, Geng P, Zhao Q.** 2020b. *Arabidopsis* MYB4 plays dual roles in flavonoid biosynthesis. *The Plant Journal* **101**, 637–652.
- Wu AM, Rihouey C, Seveno M, Höörblad E, Singh SK, Matsunaga T, Ishii T, Lerouge P, Marchant A.** 2009. The *Arabidopsis* IRX10 and IRX10-LIKE glycosyltransferases are critical for glucuronoxylan biosynthesis during secondary cell wall formation. *The Plant Journal* **57**, 718–731.
- Yoo SD, Cho YH, Sheen J.** 2007. *Arabidopsis* mesophyll protoplasts: a versatile cell system for transient gene expression analysis. *Nature Protocols* **2**, 1565–1572.
- Yue F, Lu F, Sun RC, Ralph J.** 2012. Syntheses of lignin-derived thioacidolysis monomers and their uses as quantitation standards. *Journal of Agricultural and Food Chemistry* **60**, 922–928.
- Zhao Q, Dixon RA.** 2011. Transcriptional networks for lignin biosynthesis: more complex than we thought? *Trends in Plant Science* **16**, 227–233.
- Zhao Q, Wang H, Yin Y, Xu Y, Chen F, Dixon RA.** 2010. Syringyl lignin biosynthesis is directly regulated by a secondary cell wall master switch. *Proceedings of the National Academy of Sciences, USA* **107**, 14496–14501.
- Zhao X, Jiang Y, Li J, Huq E, Chen ZJ, Xu D, Deng XW.** 2018. COP1 SUPPRESSOR 4 promotes seedling photomorphogenesis by repressing CCA1 and PIF4 expression in *Arabidopsis*. *Proceedings of the National Academy of Sciences, USA* **115**, 11631–11636.
- Zhong R, Demura T, Ye ZH.** 2006. SND1, a NAC domain transcription factor, is a key regulator of secondary wall synthesis in fibers of *Arabidopsis*. *The Plant Cell* **18**, 3158–3170.
- Zhong R, Lee C, Ye ZH.** 2010. Global analysis of direct targets of secondary wall NAC master switches in *Arabidopsis*. *Molecular Plant* **3**, 1087–1103.
- Zhong R, Lee C, Zhou J, McCarthy RL, Ye ZH.** 2008. A battery of transcription factors involved in the regulation of secondary cell wall biosynthesis in *Arabidopsis*. *The Plant Cell* **20**, 2763–2782.
- Zhong R, Richardson EA, Ye ZH.** 2007. Two NAC domain transcription factors, SND1 and NST1, function redundantly in regulation of secondary wall synthesis in fibers of *Arabidopsis*. *Planta* **225**, 1603–1611.
- Zhong R, Ye ZH.** 2012. MYB46 and MYB83 bind to the SMRE sites and directly activate a suite of transcription factors and secondary wall biosynthetic genes. *Plant & Cell Physiology* **53**, 368–380.
- Zhong R, Ye ZH.** 2015. The *Arabidopsis* NAC transcription factor NST2 functions together with SND1 and NST1 to regulate secondary wall biosynthesis in fibers of inflorescence stems. *Plant Signaling & Behavior* **10**, e989746.
- Zhou J, Lee C, Zhong R, Ye ZH.** 2009. MYB58 and MYB63 are transcriptional activators of the lignin biosynthetic pathway during secondary cell wall formation in *Arabidopsis*. *The Plant Cell* **21**, 248–266.
- Zhou J, Zhong R, Ye ZH.** 2014. *Arabidopsis* NAC domain proteins, VND1 to VND5, are transcriptional regulators of secondary wall biosynthesis in vessels. *PLoS One* **9**, e105726.